Theory of the two-photon micromaser: Photon statistics

Imrana Ashraf, J. Gea-Banacloche,* and M. S. Zubairy
Department of Electronics, Quaid-i-Azam University, Islamabad, Pakistan
(Received 6 July 1990)

Exact results for the photon statistics of a two-photon micromaser are presented, including the effect of finite detuning of the intermediate level. A periodic dependence on interaction times is shown to arise for large detunings, when sufficiently long interaction times are considered. Some typical photon-number distributions are shown, including some exhibiting sub-Poissonian fluctuations and multiple peaks. Previous treatments and the validity of some usual approximations are discussed. By direct comparison with the exact results, it is shown that the effective-Hamiltonian approximation yields incorrect equations for the off-diagonal elements of the field density matrix.

I. INTRODUCTION

Two-photon processes are extremely interesting in quantum optics, for the high degree of correlation between the photons in a pair may lead to the generation of nonclassical states of the electromagnetic field, such as number states,[1] or squeezed states,[2] or to violations of classical expectations in interference experiments.[3] Quite recently, a two-photon micromaser has been operated.[4] This system offers a unique chance to study under controlled conditions the interaction of a single mode of the electromagnetic field with a source of correlated pairs of photons.

The theory of the two-photon micromaser was first presented by Brune *et al.*[5] and Davidovich *et al.*[6] Recently, two of the present authors reported results for the photon statistics of the two-photon micromaser[7] which appear to be at variance with some of the conclusions of Ref. 6. Our purpose here is to explain this apparent discrepancy and to present a comprehensive study of the photon statistics of the two-photon micromaser, including long interaction times, and finite detuning of the intermediate level.

Our treatment will be based on the exact solution for a three-level cascade atomic system interacting with a single-mode radiation field. As the intermediate level is detuned from one-photon resonance, a two-photon transition results. We shall show here how this happens and how the photon statistics evolves, as the detuning is increased, from a behavior very similar to the conventional one-photon micromaser[8,9] to the characteristic two-photon pattern reported in Ref. 7. We shall also investigate the range of validity of some of the approximations normally made in the study of two-photon processes, by comparing the exact solution for the three-level system to the usual "effective-Hamiltonian" treatments.

Our paper is organized as follows. In Sec. II the model is introduced, the equation of motion for the field density matrix is derived, and the general solution for the diagonal elements is given. In Sec. III the "two-photon cascade micromaser," i.e., the limit of vanishing detuning of the intermediate level from exact one-photon resonance, is discussed and compared to the ordinary one-photon micromaser. In Sec. IV the transition to a true two-photon micromaser as the detuning is increased is shown both graphically and analytically; the photon statistics of the two-photon micromaser are discussed, a number of features are explained, and the range of validity of the various approximations is clarified.

II. DENSITY MATRIX EQUATIONS OF MOTION FOR A THREE-LEVEL TWO-PHOTON MICROMASER

The system we shall consider is a three-level cascade as illustrated in Fig. 1, coupled to a single mode of the electromagnetic field of frequency $\omega=(\omega_a-\omega_c)/2$; that is, exact two-photon resonance is assumed throughout. The detuning of the middle level $|b\rangle$ from exact *one*-photon resonance is

$$\Delta=\omega-(\omega_a-\omega_b)=(\omega_b-\omega_c)-\omega \tag{1}$$

(where the energies of the atomic levels are $E_{a,b,c}=\hbar\omega_{a,b,c}$). In practice, the Rydberg states of alkali-metal atoms provide this kind of level structure with varying degrees of detuning of the intermediate level

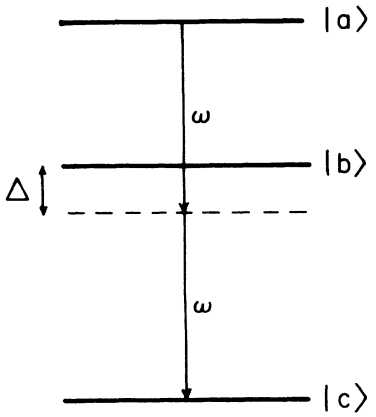

FIG. 1. Scheme of the level structure considered. Other levels are assumed to be very far off-resonance with the transitions at frequency ω.

(see Refs. 4–6). If $\Delta=0$ one has merely two one-photon transitions, whereas for Δ large enough, as we shall see below, the transition acquires a two-photon character.

The Hamiltonian in the interaction picture is

$$V_I=\hbar g_1(a|a\rangle\langle b|e^{-i\Delta t}+a^\dagger|b\rangle\langle a|e^{i\Delta t}) +\hbar g_2(a|b\rangle\langle c|e^{i\Delta t}+a^\dagger|c\rangle\langle b|e^{-i\Delta t}) , \tag{2}$$

where g_1 and g_2 are the one-photon coupling constants for the transitions $|a\rangle\rightarrow|b\rangle$ and $|b\rangle\rightarrow|c\rangle$, respectively. The lifetime of all the levels will be assumed to be much larger than the interaction time of each atom with the field in the maser cavity. Then the spontaneous decay processes to other levels or other modes may be neglected, which means that the joint evolution of the single-mode field and atom is unitary.

We shall assume that the atoms are injected into the cavity so that there is never more than one atom present at the same time. Let an atom be injected in the upper state $|a\rangle$ at time t_0. The total density operator for the atom-field system at that time is

$$\rho_T(t_0)=|a\rangle\langle a|\otimes\rho_F =\sum_{n,m}[\rho_F(t_0)]_{nm}|a,n\rangle\langle a,m| , \tag{3}$$

where ρ_F is the density operator for the field alone. Because the evolution is unitary, the total density operator at a later time $t=t_0+\tau$ may be written as

$$\rho_T(t)=\sum_{n,m}[\rho_F(t_0)]_{nm}|\psi_n(t)\rangle\langle\psi_m(t)| , \tag{4}$$

where $|\psi_n(t)\rangle$ is the solution of the Schrödinger equation

$$\frac{\partial}{\partial t}|\psi_n(t)\rangle=-\frac{i}{\hbar}V_I|\psi_n(t)\rangle \tag{5}$$

subject to the initial condition

$$|\psi_n(t_0)\rangle=|a,n\rangle . \tag{6}$$

A moment's inspection of the Hamiltonian (2) shows that $|\psi_n(t)\rangle$ must be of the form

$$|\psi_n(t)\rangle=C_{a,n}|a,n\rangle+C_{b,n+1}|b,n+1\rangle +C_{c,n+2}|c,n+2\rangle . \tag{7}$$

When Eq. (7) is substituted in Eq. (5) one obtains the following closed system of equations:

$$\dot{C}_{an}(t)=-ig_1\sqrt{n+1}\,e^{-i\Delta t}C_{b,n+1}(t) , \tag{8a}$$

$$\dot{C}_{b,n+1}(t)=-ig_1\sqrt{n+1}\,e^{i\Delta t}C_{an}(t) -ig_2\sqrt{n+2}\,e^{i\Delta t}C_{c,n+2}(t) , \tag{8b}$$

$$\dot{C}_{c,n+2}(t)=-ig_1\sqrt{n+2}\,e^{-i\Delta t}C_{b,n+1}(t) , \tag{8c}$$

whose solution, subject to the initial condition (6), is

$$C_{an}(t_0+\tau)=\frac{g_1^2(n+1)}{\beta_n\alpha_n^2}\left[\beta_n\cos\beta_n\tau+i\frac{\Delta}{2}\sin\beta_n\tau-\beta_n e^{i\Delta\tau/2}\right]e^{-i\Delta\tau/2}+1 , \tag{9a}$$

$$C_{b,n+1}(t_0+\tau)=-i\frac{g_1\sqrt{n+1}}{\beta_n}e^{i\Delta t_0}e^{i\Delta\tau/2}\sin\beta_n\tau , \tag{9b}$$

$$C_{c,n+2}(t_0+\tau)=\frac{g_1g_2\sqrt{(n+1)(n+2)}}{\beta_n\alpha_n^2}\left[\beta_n\cos\beta_n\tau+i\frac{\Delta}{2}\sin\beta_n\tau-\beta_n e^{i\Delta\tau/2}\right]e^{-i\Delta\tau/2} , \tag{9c}$$

where $\tau=t-t_0$ is the interaction time and Rabi frequencies α_n and β_n are

$$\alpha_n=[g_1^2(n+1)+g_2^2(n+2)]^{1/2} , \tag{10a}$$

$$\beta_n=\left[\frac{\Delta^2}{4}+\alpha_n^2\right]^{1/2} . \tag{10b}$$

We may now use solution (9) in Eq. (7), and this, in turn, in Eq. (4), to obtain an expression for the evolution of the total density matrix $\rho(t)$ over the interaction time τ. We assume that at the end of this time the atom leaves the cavity. The new reduced density matrix for the field alone is obtained by tracing over the atomic states and has the form

$$[\rho_F(t_0+\tau)]_{nm}=[\rho_F(t_0)]_{nm}C_{an}(t_0+\tau)C_{am}^*(t_0+\tau)+[\rho_F(t_0)]_{n-1,m-1}C_{bn}(t_0+\tau)C_{bm}^*(t_0+\tau) +[\rho_F(t_0)]_{n-2,m-2}C_{cn}(t_0+\tau)C_{cm}^*(t_0+\tau) . \tag{11}$$

This difference equation may be approximated by a differential equation, as is done in standard laser theory, assuming that the average time interval between successive atoms is Δt and thus that the rate of injection $r_a=1/\Delta t$,

$$\dot{\rho}_{nm}\simeq\frac{\rho_{nm}(t+\tau)-\rho_{nm}(t)}{\Delta t}=r_a\delta\rho_{nm} , \tag{12}$$

where

$$\delta\rho_{nm}=\rho_{nm}(t+\tau)-\rho_{nm}(t) \tag{13}$$

and the subscripts 0 and F have been dropped from t_0 and ρ_F, respectively, for convenience. The total rate of change of the field density matrix is obtained by adding to Eq. (12) the cavity-loss terms in the standard way.[10]

The final result has the form

$$\dot{\rho}_{nm}=a_{nm}\rho_{nm}+b_{n-1,m-1}\rho_{n-1,m-1}+d_{n-2,m-2}\rho_{n-2,m-2}+c_{n+1,m+1}\rho_{n+1,m+1}\ , \tag{14}$$

where

$$a_{nm}=r_a(C_{an}C^*_{am}-1)-\frac{\gamma}{2}[2\bar{n}_b(n+m+1)+n+m]\ , \tag{15a}$$

$$b_{nm}=r_a C_{b,n+1}C^*_{b,m+1}-\gamma\bar{n}_b[(n+1)(m+1)]^{1/2}\ , \tag{15b}$$

$$c_{nm}=\gamma(\bar{n}_b+1)\sqrt{nm}\ , \tag{15c}$$

$$d_{nm}=r_a C_{c,n+2}C^*_{c,m+2}\ . \tag{15d}$$

Here γ is the (intensity) cavity-loss rate, sometimes written as ν/Q, and $\bar{n}_b$ is the average number of photons in thermal equilibrium, in the absence of interaction with the atoms. The expressions for C_{an}, C_{bn}, and C_{cn} are those in Eqs. (9), where τ is the interaction time [note that the dependence on t_0 vanishes from Eq. (15)].

We may now set $n=m$ and look at the field photon statistics. At steady state, the probability $P(n)=\rho_{nn}$ to find n photons inside the cavity satisfies the equation

$$a_nP(n)+b_{n-1}P(n-1)+c_{n+1}P(n+1)+d_{n-2}P(n-2)=0 \tag{16}$$

(where $a_n\equiv a_{nn}$, and so forth). Unlike the ordinary laser or the one-photon micromaser, here no detailed-balance condition holds. Nevertheless, it is possible to derive a closed-form solution to Eq. (16) as a product of continued fractions, along the same lines as shown in Refs. 7 and 11. Noting that

$$a_n+b_n+c_n+d_n=0 \tag{17}$$

we find

$$P(n)=P(0)\prod_{r=1}^{n}\frac{1}{c_r}\left[b_{r-1}+d_{r-1}+\cfrac{d_{r-2}c_{r-1}}{b_{r-2}+d_{r-2}+\cfrac{d_{r-3}c_{r-2}}{\ddots\cfrac{}{b_1+d_1+\cfrac{d_0c_1}{b_0+d_0}}}}\right]\ . \tag{18}$$

This is our basic result. In the following sections we study the photon statistics predicted by Eq. (18) for a number of cases of interest. Section II is devoted to the case of a "two-photon cascade micromaser," with $\Delta=0$, which has not been considered previously in the literature. Section III discusses the "true two-photon micromaser," i.e., the case of $\Delta\neq 0$ and, in particular, $\Delta/g\sqrt{n}\gg 1$.

III. TWO-PHOTON CASCADE MICROMASER

In this section we study the photon statistics of the three-level micromaser for exact one-photon resonance, $\Delta=0$ (such near resonances may be found for chosen transitions in Rydberg alkali atoms; see Ref. 5). The two-photon process reduces then to just two one-photon transitions, and our results look very similar to those which have been predicted for the one-photon micromaser,[8,9] except for the almost complete absence of "trapping states," as will be discussed presently.

We shall assume throughout, for simplicity, that the magnitude of the matrix elements for the two transitions is approximately the same, that is,

$$g_1=g_2\equiv g\ . \tag{19}$$

We shall also follow the usual practice of introducing a measure of the pumping rate normalized to the cavity decay rate, $N_{\rm ex}$,

$$N_{\rm ex}=\frac{r_a}{\gamma}\ . \tag{20}$$

Figure 2 shows $\langle n\rangle$, the average number of photons, and σ, the photon number standard deviation, normalized to its value for a Poisson distribution,

$$\sigma=\left[\frac{\langle n^2\rangle-\langle n\rangle^2}{\langle n\rangle}\right]^{1/2}\ , \tag{21}$$

as a function of $g\tau$, the normalized interaction time, for zero temperature ($\bar{n}_b=0$) and for the pumping rate $N_{\rm ex}=20$. The behavior of $\langle n\rangle$ in Fig. 2(a) is very similar to the corresponding one for the one-photon micromaser obtained by Wright and Meystre:[9] there is a "collapse" followed by a single, undecaying revival. The structure is quite irregular. The effect of increasing temperature is also similar to that found in Ref. 9: see Fig. 3, which is calculated for $n_b=5$. The "collapse" becomes more distinct and the oscillations are somewhat smoothed.

Regarding the standard deviation σ, one can see from Fig. 2(b) that sub-Poissonian statistics ($\sigma<1$) are possible at low temperatures, in some cases corresponding to relatively large average values of the photon number. It is perhaps noteworthy that in the "collapse" region in Fig. 2(b) the field appears to be very nearly Poissonian. Figure 3(b) shows the effect of increasing the temperature: already for $n_b=5$, the nonclassical fluctuations have disappeared and the distribution is super-Poissonian for all values of τ.

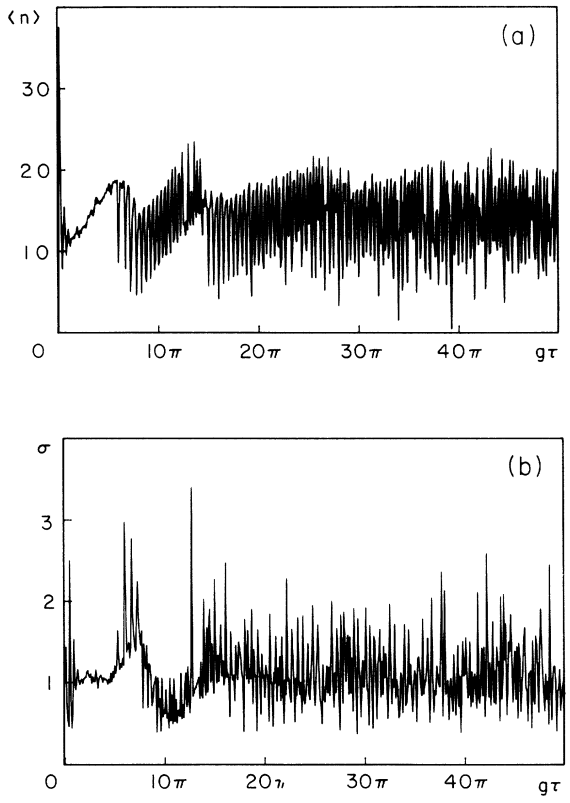

FIG. 2. Steady-state properties of the cascade micromaser, $\Delta=0$, for an excitation rate $N_{ex}=20$, and at zero temperature ($\bar{n}_b=0$). (a) Average number of photons vs dimensionless interaction time, $g\tau$. (b) Normalized variance $\sigma=(\langle n\rangle^2-\langle n^2\rangle)^{1/2}/\langle n\rangle^{1/2}$ vs $g\tau$.

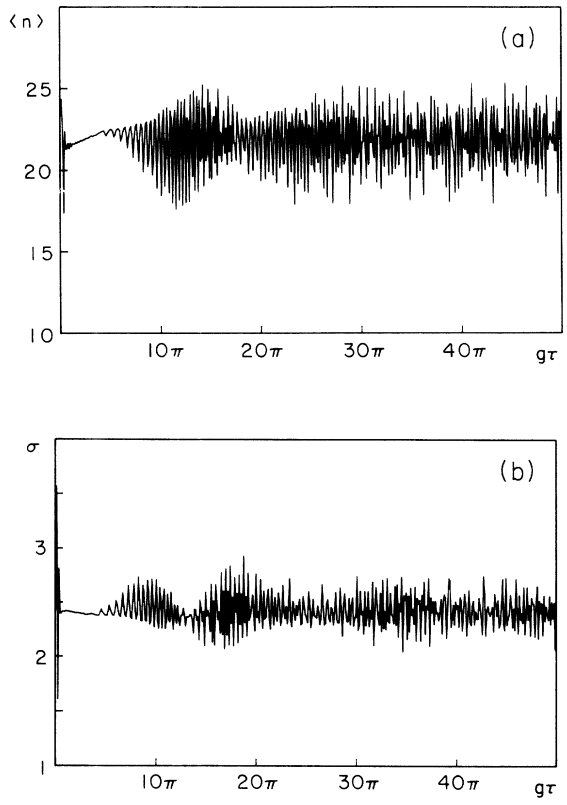

FIG. 3. Cascade micromaser at finite temperature, $\bar{n}_b=5$. All other parameters as in Fig. 2.

Trapping states[8] can be seen in the expanded view of the collapse region shown in Fig. 4. One of the major differences between the present system and the one-photon micromaser is that in the present case there is only one sequence of trapping states, all corresponding to $|n\rangle=|0\rangle$. The reason is that a transition upward in photon number (from, say, state $|n\rangle$) may take place by the emission of either one or two photons. These two events have probabilities proportional to the coefficients b_{nn} and d_{nn} of Eq. (14), respectively. By Eqs. (15) and (9), at zero temperature (and $\Delta=0$) we have

$$b_{nn}\sim\sin^2\alpha_n\tau\ , \tag{22a}$$

$$d_{nn}\sim\sin^4(\alpha_n\tau/2)\ . \tag{22b}$$

It is in principle possible to make both (22a) and (22b) vanish simultaneously, for any n, by a proper choice of τ, but it does not follow that the state $|n\rangle$ becomes then a barrier, as it would in the one-photon micromaser. For there is always some probability for the (one-photon) losses to bring the photon number down by one, to the state $|n-1\rangle$, and then the atom has some probability, $d_{n-1,n-1}$, proportional to

$$\sin^4(\alpha_{n-1}\tau/2) \tag{23}$$

to emit *two* photons and jump over the barrier, to the state $|n+1\rangle$. It is in general impossible for any n to make all three of the probabilities (22) and (23) vanish simultaneously when α_n is given by Eq. (10a).

All this means is that there is really only one trapping state, namely, the vacuum $|n=0\rangle$, for which the one- and two-photon transition probabilities vanish when

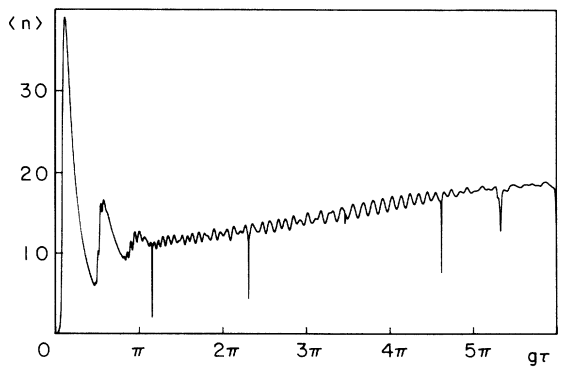

FIG. 4. Expanded view of Fig. 2(a) for short interaction times showing "trapping states": $\Delta=0$, $N_{ex}=20$, $\bar{n}_b=0$.

$$\alpha_0\tau = 2q\pi \tag{24}$$

where q is an integer; that is,

$$g\tau = 0, \frac{2\pi}{\sqrt{3}}, \frac{4\pi}{\sqrt{3}}, \ldots, \tag{25}$$

which yields a periodic sequence of trapping "resonances," as seen in Fig. 4, for zero temperature ($\bar{n}_b = 0$). [There is one state missing from Fig. 4, at $6\pi/\sqrt{3} \simeq 10.9$; this is due to the finite resolution with which the points were sampled, which is also the reason why the dips do not reach all the way to zero. This is an indication of the extreme narrowness of these features. Note also that the dip on the far right of Fig. 4, near $g\tau = 16.8$, is not one of the trapping states (25); the origin of this particular feature is not clear.]

At higher temperatures, of course, $|0\rangle$ loses its trapping character as well, since thermal fluctuations may take the field to the state $|1\rangle$, from where the photon number may continue to increase. This is quite analogous to the vanishing of the trapping resonances as $\bar{n}_b$ increases in the one-photon micromaser.[8]

The absence of trapping states suggests that one could not, in principle, use the two-photon micromaser to generate a number state dynamically, a possibility which has been suggested instead for the one-photon micromaser[12] at very low temperatures. (The scheme of number state generation by state reduction proposed by Krause, Scully, and Walther,[13] however, might still be applicable.)

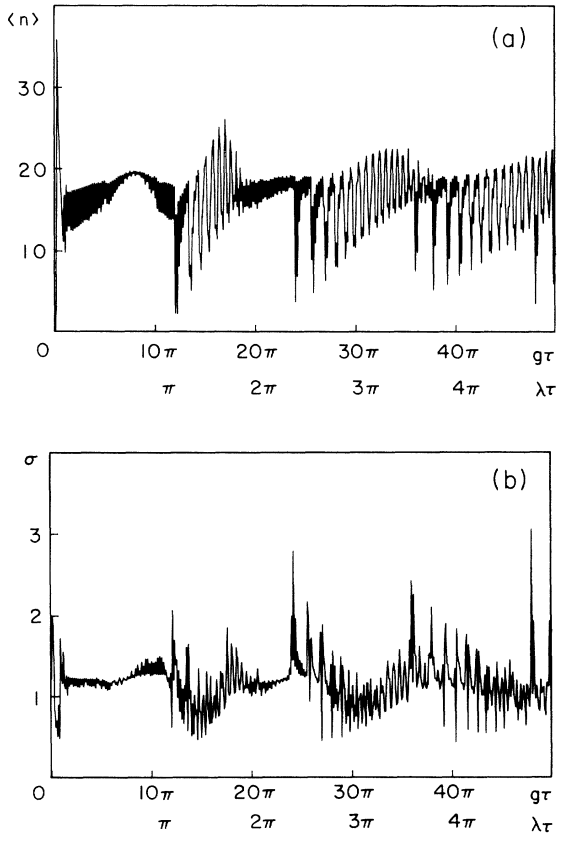

FIG. 5. Steady-state properties of a two-photon micromaser with finite detuning of the intermediate level, $\Delta = 10g$. All other parameters as in Fig. 2. (a) Average photon number, (b) normalized variance. The second scale on the horizontal axis, in units of $\lambda\tau$, is included to facilitate the comparison with the large-detuning case (Fig. 6); $\lambda = g^2/\Delta$ is the effective two-photon coupling constant.

IV. THE TRUE TWO-PHOTON MICROMASER

Figures 5 and 6 show the dependence of $\langle n \rangle$ and σ on $g\tau$ for a finite detuning: $\Delta = 10g$ and $\Delta = 50g$, respectively. Clearly Fig. 6 already exhibits the regular, periodic features expected from a true two-photon transition (compare Ref. 7), whereas Fig. 5 may be seen to fall between this and the $\Delta = 0$ case of Fig. 2: the first period is just beginning to take shape.

In this section we shall first establish how this limit is approached analytically; then we shall look at the photon number distributions corresponding to Fig. 6 in greater detail; and finally we shall consider the question of the different approximations to the descriptions of two-photon processes.

A. The limit of large detuning

Analytically the limit of large detuning is not hard to obtain from the exact solutions (9) to the atom-field evolution equations. Under the condition

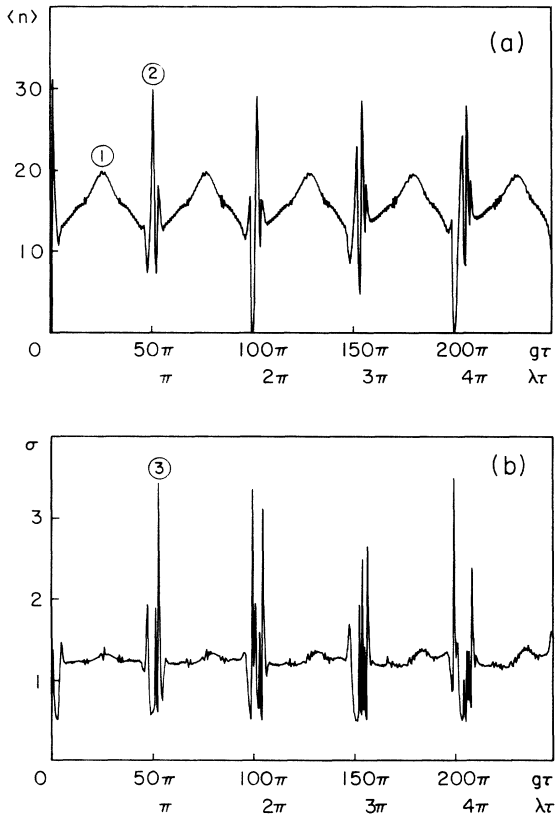

FIG. 6. All parameters as in Figs. 2 and 5 except for the detuning, $\Delta = 50g$. The numbers refer to particular values of the interaction time for which the corresponding photon number distributions are plotted in full in Fig. 8.

$$8\frac{g^2 n}{\Delta^2} \ll 1 \tag{26}$$

the frequency β_n, given by Eq. (10), may be expanded as

$$\beta_n = \left[\frac{\Delta^2}{4} + g^2(2n+3)\right]^{1/2} \simeq \frac{\Delta}{2} + \frac{g^2}{\Delta}(2n+3) . \tag{27}$$

In this limit clearly the coefficient C_{bn} of Eq. (9b) is (almost always, see below) much smaller than C_{an} and C_{cn}. This means that the probability to find the system in state $|b\rangle$ becomes negligible. At the same time, the one-photon transition probability b_{nn} in Eq. (15b) becomes (except for the contribution of the thermal fluctuations) negligible versus the two-photon transition probability d_{nn} [Eq. (15d)].

More quantitatively, let us introduce an effective two-photon coupling constant λ as

$$\lambda = \frac{g^2}{\Delta} . \tag{28}$$

Let also

$$\epsilon = \frac{2\lambda}{\Delta}(2n+3) . \tag{29}$$

Then if $\epsilon \ll 1$, we may write

$$C_{an} = 1 + \frac{n+1}{2n+3}(e^{i\lambda(2n+3)\tau} - 1) - \frac{\epsilon}{2}\frac{n+1}{2n+3}(e^{i\lambda(2n+3)\tau} - e^{-i[\Delta+\lambda(2n+3)]\tau}) , \tag{30a}$$

$$C_{b,n+1} = \frac{g\sqrt{n+1}}{\Delta(1+\epsilon)} e^{i\Delta t_0}(e^{-i\lambda(2n+3)\tau} - e^{i[\Delta+\lambda(2n+3)]\tau}) \sim \sqrt{\epsilon} , \tag{30b}$$

$$C_{c,n+2} = \frac{\sqrt{(n+1)(n+2)}}{2n+3}(e^{i\lambda(2n+3)\tau} - 1) + \frac{\epsilon}{2}(e^{i\lambda(2n+3)\tau} - e^{-i[\Delta+\lambda(2n+3)]\tau}) . \tag{30c}$$

If the terms of order ϵ are ignored everywhere [note that $C_{b,n}$ is to be squared in the density matrix equation, Eq. (11); see Eqs. (14) and (15b)] the transition amplitudes C_{an} and $C_{c,n+2}$, Eqs. (30a) and (30c), may be directly compared to Eqs. (2.11) and (2.12) of Ref. 6. In this limit all the predictions of the theory are periodic in τ with period $2\pi/\lambda$. Figure 6, for which $\Delta/g = 50$ and thus $\epsilon \sim 4\langle n\rangle/2500 \sim 0.03$, exhibits this periodicity, whereas Fig. 5, for which $\Delta/g = 10$ and thus $\epsilon \sim 0.8$, does not. (Note the change in the horizontal scale from Fig. 5 to Fig. 6, so that both cover the same range of values of $\lambda\tau$, i.e., the same number of periods.)

Only the leading terms in Eqs. (30) are periodic with period $2\pi/\lambda$ irrespective of the value of n. Thus, near the points where these terms vanish, i.e., near

$$\tau = \frac{2q\pi}{\lambda}, \quad q = 1,2,3,\ldots , \tag{31}$$

deviations from strict $2\pi/\lambda$ periodicity will be apparent, as indeed they are in Fig. 6. Figure 6 also shows that the periodicity is less accurately obeyed for longer interaction times. This is because the argument of the trigonometric functions appearing in the original probability amplitudes (9) is $\beta_n\tau$; thus, for a sufficiently large value of τ it is incorrect to replace β_n by the approximate expression (27) in the argument of the trigonometric functions.

It is easy to show that the requirement for the approximation (27) to be legitimate in the trigonometric functions is

$$4n^2\left[\frac{g}{\Delta}\right]^2 \lambda\tau \ll 1 , \tag{32a}$$

or, if $n = 0, 1$,

$$9\left[\frac{g}{\Delta}\right]^2 \lambda\tau \ll 1 . \tag{32b}$$

In the case of Fig. 6, with $n \simeq 20$ and $g/\Delta = \frac{1}{50}$, the inequality (32a) is not satisfied over the whole range plotted; still, the approximate periodicity is clearly visible.

The experiments reported in Ref. 4 had $\Delta/g \simeq 350$ and $g \simeq 7\times 10^5$ s^{-1}, so that $\lambda = g^2/\Delta = 2\times 10^3$ s^{-1}. To observe a couple of periods of $2\pi/\lambda$, as in Fig. 6, the interaction time would have to be of the order of 6 ms. The field decay time in the cavity, however, is only of the order of 0.2 ms, so it would not be justified to neglect the cavity losses during the interaction time. In fact, it would probably be impossible to achieve any significant field intensity under these conditions, unless one had many atoms in the cavity simultaneously. It appears, then, that to observe the approximate periodicity exhibited in Fig. 6—which is a genuine two-photon effect—larger values of λ would be necessary, which might be reached in atomic systems for which the detuning Δ of

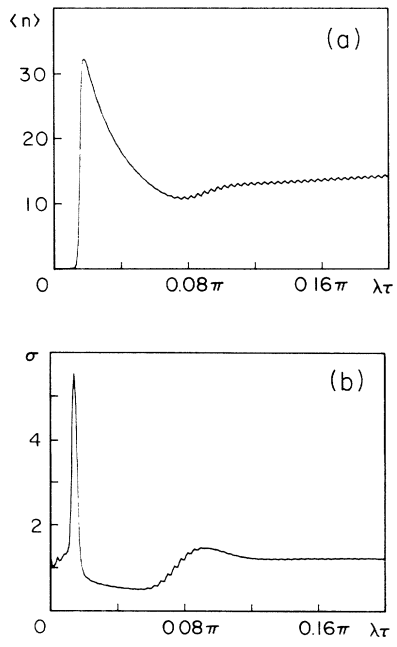

FIG. 7. Expanded view of Fig. 6 showing the region of small interaction times.

the intermediate system were smaller than for the system in Ref. 4 [although still large enough for two-photon effects to dominate, i.e., for Eq. (26) to be valid].

In principle, the authors of Ref. 6 would have obtained (exact) periodicity from the numerical solution of their master equation if they had considered long enough interaction times. This periodicity was lost, however, in their analytical treatment, since they made n a continuous variable and also expanded the trigonometric functions in powers of the quantity $3\lambda\tau$, to first order (which is clearly not justified for sufficiently larger τ, but which would be acceptable for the experiments of Ref. 4, where $\tau \simeq 25\ \mu$s).

Graphs of $\langle n \rangle$ and σ for short interaction times are shown in Fig. 7. They may be seen to look very similar to those obtained numerically in Ref. 6, from a master equation which essentially contains only the leading terms ($\epsilon=0$) in the expansion (30).

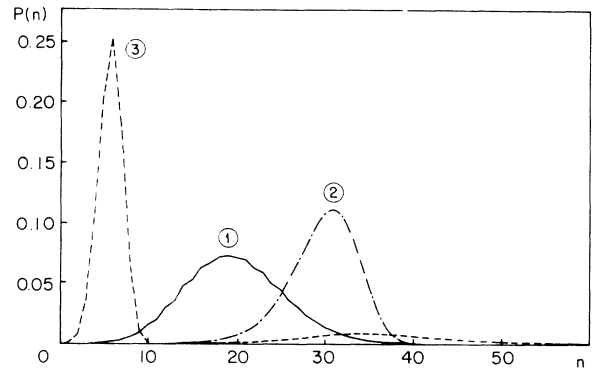

FIG. 8. Steady-state photon number distributions corresponding to the points marked in Figs. 6(a) and 6(b). In all cases $\Delta=50g$, $\bar{n}_b=0$, $N_{ex}=20$. The values of $\lambda\tau$ for the three curves are (1) $\lambda\tau=0.51\pi$ (solid line); (2) $\lambda\tau=1.02\pi$ (dash-dotted line); (3) $\lambda\tau=1.06\pi$ (dashed line, double-peaked). See text for more details.

B. Photon statistics for large detuning

In this subsection we shall look in more detail at some of the features of the large-detuning limit (Fig. 6); in particular, the trapping states and some of the photon number distributions.

1. *Trapping states*

One may expect that for this system also there would be no trapping states, for the same reasons that were given for the cascade system in Sec. II, except perhaps for the vacuum state $|0\rangle$. In fact, for this system, not even the vacuum is in general a trapping state. It may be checked easily from expression (9) for the transition amplitudes that, in general, when $\Delta\neq 0$ it is not possible to make both $C_{b1}=0$ and $C_{c2}=0$ simultaneously, which would be necessary for the system to be trapped in the state $|0\rangle$ at zero temperature [as may be seen from the general form of the state vector (7)].

On the other hand, in the approximate expression (30c) for C_{c2} the leading term vanishes for $\tau=2q\pi/\lambda$, making the probability to leave the vacuum state by emission of two photons very small. The probability of emission of just one photon is also very small in this large-detuning limit, and hence the dips at $\tau=2\pi/\lambda$, $4\pi/\lambda$ in Fig. 6. [In fact, for the case plotted in Figs. 5 and 6, there is an additional, accidental vanishing of higher-order terms in Eqs. (30c) and (30b) at the same points, which results from our having chosen an integer value for Δ/g.]

Note that the trapping states found in Ref. 7 are also absent from the present, more exact treatment. (A discussion of the relationship between the present treatment and that in Ref. 7 will be found later in this section.)

2. *Photon number distributions*

It is somewhat remarkable that, as Fig. 6(b) shows, the normalized variance of the photon number distribution is rather close to the value of 1 for most values of τ. This does not, however, imply that the photon number distribution is necessarily Poissonian, or even close to it.

Figure 8 displays the photon number distributions $P(n)$ for some chosen values of τ, labeled on Fig. 6. Curve 1 corresponds to $\lambda\tau=0.51\pi$, one of the local maxima in Fig. 6(a), and has $\langle n \rangle=19.9$ and $\sigma=1.25$. (The reason one might expect $\langle n \rangle \sim N_{ex}$ in general has been discussed in Ref. 6.) Curve 2 corresponds to a higher peak in Fig. 6(a), at $\lambda\tau=1.02\pi$, for which $\langle n \rangle=29.8$, and is sub-Poissonian with $\sigma=0.695$. Curve 3 corresponds to $\lambda\tau=1.06\pi$, and is instead super-Poissonian ($\sigma=3.44$) and double-peaked (there are still smaller secondary maxima not visible in the figure), with $\langle n \rangle=9.9$; it corresponds to one of the peaks in Fig. 6(b).

Figure 9 shows a particularly curious "rarity": a double-peaked photon number distribution with nonetheless a *sub*-Poissonian variance, $\sigma=0.8$. It corresponds to $\lambda\tau=1.95\pi$, another of the "pathological" regions of Fig. 6. All the sub-Poissonian distributions obtained around that particular "dip" of Fig. 6(b) are, in fact, multiple-peaked.

Still other types of distributions are possible; we have found some which look like curve 1 in Fig. 8, but with a

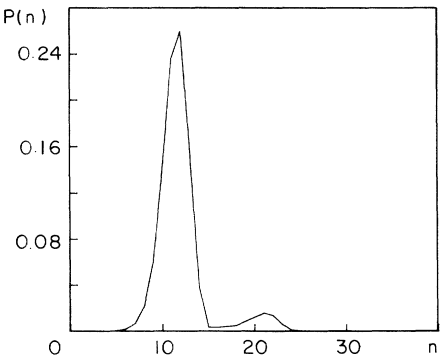

FIG. 9. Steady-state photon number distribution for $\lambda\tau=1.95\pi$ (other parameters as in Fig. 8). This double-peaked distribution has a sub-Poissonian variance, $\sigma=0.8$ ($\langle n \rangle=12.0$).

"jagged" top, for instance (this is the case, in particular, at $\lambda\tau=\pi/2$). The multiple-peaked distributions are also not confined to large values of τ: they are found in the region plotted in Fig. 7 as well. The distributions around the second maximum of Fig. 7(b), for instance, are fairly bimodal: that is, they exhibit two distinct peaks of comparable height.

While these multiple peaks must be related to the multistability already predicted in the semiclassical limit in Ref. 5, we have not attempted to establish a detailed correspondence with this theory (nor with the more accurate quantum potential theory of Ref. 6). We note only that the existence of these bimodal distributions makes questionable the validity of the semiclassical approach of replacing n by $\langle n \rangle$; this may have important consequences, e.g., in linewidth calculations.

C. The effective-Hamiltonian approximation. Off-diagonal elements

The purpose of this subsection is to compare our exact results with one of the most frequently used approximations in the study of two-photon processes, namely, the "effective-Hamiltonian" approach, where one considers just the two-level system $|a\rangle$, $|c\rangle$, with a Hamiltonian

$$V_I=\hbar\lambda(|c\rangle\langle a|a^2+a^{\dagger 2}|a\rangle\langle c|) . \tag{33}$$

Proceeding in the usual way, one may derive from this Hamiltonian an equation of motion for the reduced density matrix for the field inside the cavity which is formally analogous to (14), but with

$$a'_{nm}=r_a(C'_{an}C'^{*}_{am}-1)-\frac{\gamma}{2}[2\bar{n}_b(n+m+1)+n+m] , \tag{34a}$$

$$b'_{nm}=r_a C_{b,n+1}C^{*}_{b,m+1}-\gamma\bar{n}_b[(n+1)(m+1)]^{1/2} , \tag{34b}$$

$$c'_{nm}=\gamma(\bar{n}_b+1)\sqrt{nm} , \tag{34c}$$

$$d'_{nm}=r_a C'_{c,n+2}C'^{*}_{c,m+2} , \tag{34d}$$

where

$$C'_{an}=\cos(\beta'_n\tau/2) , \tag{35a}$$

$$C'_{c,n+2}=-i\sin(\beta'_n\tau/2) , \tag{35b}$$

with

$$\beta'_n=2\lambda[(n+1)(n+2)]^{1/2} . \tag{36}$$

This is to be compared to the large-detuning limit of our exact result, i.e., with Eqs. (15) with (27)–(30), which looks in general rather different. A limited agreement is obtained in the case when the number of photons, n, is large. Then we can write

$$\beta'_n\simeq\lambda(2n+3) \tag{37}$$

[compare with Eq. (27)] and

$$C'_{an}=\tfrac{1}{2}e^{-i\lambda(2n+3)\tau/2}(e^{i\lambda(2n+3)\tau}+1) , \tag{38a}$$

$$C'_{c,n+2}=-\tfrac{1}{2}e^{-i\lambda(2n+3)\tau/2}(e^{i\lambda(2n+3)\tau}-1) . \tag{38b}$$

If this is compared now to the large-n limit of the leading terms in Eqs. (30a) and (30c), it is seen to differ only by the phase factor $\exp[-i\lambda(2n+3)\tau/2]$. This is not a trivial phase factor, however, since it depends on n, i.e., the intensity of the field. It is, in fact, a Stark-shift term, for which the effective-Hamiltonian approach does not account properly.

We may conclude that in the calculation of the diagonal elements, where the phase factors $\exp[-i\lambda(2n+3)\tau/2]$ cancel, the difference between the effective Hamiltonian approach and the exact result (for large detuning) may be relatively small, but not so for the off-diagonal terms. In fact, for the diagonal elements, the results from the effective Hamiltonian are fairly accurate even for small n. For instance, for $n=0$, Eqs. (34d), (35b), and (36) yield $d'_{00}=r_a\sin^2(\lambda\sqrt{2}\,\tau)$ while the exact result (for very large detuning) obtained from Eqs. (15d) and (30c) is $d_{00}=\frac{8}{9}r_a\sin^2(1.5\lambda\tau)$. Of course, when the detuning is not large enough for the higher-order terms in Eqs. (30) to be negligible, the entire effective-Hamiltonian approach is not valid, and the same appears to be the case in a small region around $\lambda\tau=2q\pi$ (q an integer), where the leading terms in Eq. (30) cancel. (The width of this region naturally decreases as g/Δ.)

As regards the off-diagonal elements, we note, for instance, from Eq. (38b) and (30c), that in the limit of large n the exact $d_{nm}=C_{c,n+2}C^{*}_{c,m+2}$ and the effective-Hamiltonian $d'_{nm}=C'_{c,n+2}C'^{*}_{c,m+2}$ are approximately related by

$$d'_{nm}=e^{-i\lambda(n-m)\tau}d_{nm} . \tag{39}$$

A phase factor like this would appear also in a'_{nm}, but, of course, not in the loss terms, so it cannot simply be factored out of the equation of motion (14). This indicates that the use of the effective Hamiltonian for any calculation involving off-diagonal elements is not justified unless the interaction time is such that

$$k\lambda\tau\ll 1 , \tag{40}$$

where $k=n-m$ is the degree of off-diagonality. For linewidth calculations, typically $k=1$. We note here that in a recent study of the two-photon *laser* Boone and Swain[14] have also concluded that the effective Hamiltonian approach may yield wrong results for the off-diagonal density matrix elements.

In Ref. 6 the effective Hamiltonian is not used, and the Stark-shift phase factors are properly included; their contributions to the linewidth are, in fact, discussed there in detail.

It is interesting, on the other hand, to investigate the correctness of the treatment used in Ref. 7, which involved the adiabatic elimination of the intermediate levels, in the light of the exact results reported here. Denoting with double primes the probability amplitudes obtained in Ref. 7, and modifying the notation slightly to agree with ours, we obtain from Ref. 7

$$C''_{an}=\left[\cos(\beta''_n\tau/2)+i\frac{\omega_{n+2}}{\beta''_n}\sin(\beta''_n\tau/2)\right]e^{i\gamma_{n+2}\tau/2}, \tag{41a}$$

$$C''_{c,n+2}=\frac{2\lambda\sqrt{(n+1)(n+2)}}{\beta''_n}\sin(\beta''_n\tau/2)e^{i\gamma_{n+2}\tau/2}, \tag{41b}$$

where, for the particular three-level system illustrated in Fig. 1, the parameters γ_n, β''_n, and ω_n of Ref. 7 become

$$\gamma_n=g^2\left[\frac{2n-1}{\Delta}-\frac{n-2}{2\omega-\Delta}+\frac{n+1}{2\omega+\Delta}\right], \tag{42}$$

$$\omega_n=g^2\left[-\frac{1}{\Delta}-\frac{n-2}{2\omega-\Delta}-\frac{n+1}{2\omega+\Delta}\right], \tag{43}$$

and

$$\beta''_n=2[(\omega_{n+2}/2)^2+\lambda^2(n+1)(n+2)]^{1/2}. \tag{44}$$

This is to be compared to the leading terms of Eq. (30) (large-detuning limit), where C_{bn} is to be ignored. We may notice that if one merely sets $\gamma_n=\omega_n=0$, Eqs. (41) become identical to those derived from the effective Hamiltonian model, Eqs. (35). Equations (42) and (43), however, suggest that this is really not the right choice for this particular system, since γ_n is of the order of λn, a frequency which has been kept throughout.

A more correct approach is to realize that in the derivation of Eqs. (41)–(44) the rotating-wave approximation was *not* made, whereas it is implicit in the form of the Hamiltonian (2), from which our "exact" solution was derived. Clearly, the last two terms of Eqs. (42) and (43) are just the kind of terms which are neglected in the rotating-wave approximation; under the assumption $\omega\gg\Delta$ they may be neglected to yield (with $\lambda=g^2/\Delta$)

$$\gamma_n=\lambda(2n-1), \tag{45}$$

$$\omega_n=-\lambda. \tag{46}$$

To proceed with the comparison it seems necessary to take the limit of a large number of photons in the two-photon Rabi frequency β''_n, which yields

$$\beta''_n\simeq\lambda(2n+3). \tag{47}$$

Using Eqs. (45)–(47) in Eq. (41) one recovers *exactly* the leading terms of the exact solution, Eqs. (30a) and (30c) (except for a trivial sign). The adiabatic elimination of the middle level is thus justified by comparison with the exact solution. It is, however, somewhat mysterious at this time that the large-n limit appears to be necessary to fully establish the correspondence.

ACKNOWLEDGMENTS

J. G.-B. wishes to thank the Pakistan Atomic Energy Commission (PAEC) for financial support which made possible his visit to Quaid-i-Azam University, where most of this work was done.

*On leave of absence from Instituto de Optica, Consejo Superior de Investigaciones Científicas, Madrid, Spain. Present address: Department of Physics, University of Arkansas, Fayetteville, AR 72701.

[1]C. K. Hong and L. Mandel, Phys. Rev. Lett. **56**, 58 (1986).
[2]L-A. Wu, M. Xiao, and H. J. Kimble, J. Opt. Soc. Am. B **4**, 1465 (1987); A. Heidmann, R. J. Horowicz, S. Reynaud, E. Giacobino, C. Fabre, and G. Camy, Phys. Rev. Lett. **59**, 2555 (1987).
[3]For a very recent experiment, see Z. Y. Ou and L. Mandel, Phys. Rev. Lett. **62**, 2941 (1989); see also references therein.
[4]M. Brune, J. M. Raimond, P. Goy, L. Davidovich, and S. Haroche, Phys. Rev. Lett. **59**, 1899 (1987).
[5]M. Brune, J. M. Raimond, and S. Haroche, Phys. Rev. A **35**, 154 (1987).
[6]L. Davidovich, J. M. Raimond, M. Brune, and S. Haroche, Phys. Rev. A **36**, 3771 (1987).
[7]I. Ashraf and M. S. Zubairy, Opt. Commun. **77**, 85 (1990).
[8]P. Meystre, G. Rempe, and H. Walther, Opt. Lett. **13**, 1078 (1988).
[9]E. M. Wright and P. Meystre, Opt. Lett. **14**, 177 (1989).
[10]See, e.g., M. Sargent III, M. O. Scully, and W. E. Lamb, Jr., *Laser Physics* (Addison-Wesley, Reading, MA, 1974), Chap. 17.
[11]M. S. Zubairy, Phys. Lett. **80A**, 225 (1980).
[12]P. Filipowicz, J. Javanainen, and P. Meystre, J. Opt. Soc. Am. B **3**, 906 (1986).
[13]J. Krause, M. O. Scully, and H. Walther, Phys. Rev. A **36**, 4547 (1987).
[14]A. W. Boone and S. Swain, Quantum Opt. **1**, 27 (1989).